DIGITAL BACK PROPAGATION PERFORMANCE IN SPATIAL MULTIPLEXING SYSTEMS

Filipe M Ferreira[1]*, Stylianos Sygletos[1], Andrew D Ellis[1] and Nick J Doran[1]

[1] Aston Institute of Photonic Technologies, Aston University, Birmingham, B47ET, United Kingdom
** f.ferreira@aston.ac.uk*

Keywords: SPATIAL DIVISION MULTIPLEXING, DIGITAL BACK PROPAGATION.

Abstract

We review digital methods to mitigate the Kerr nonlinearity in multi-mode and/or multi-core fibres operating in different operational regimes as determined by differential mode delay and linear mode coupling. The results demonstrate that transmission performance can be more than doubled for feasible fibres characteristics.

1 Introduction

Spatial-division multiplexing (SDM) has emerged as one possible solution to overcome the capacity limit of single-mode fibres (SMFs) [1]. Among the SDM approaches offering the highest spatial information density there are two prime candidates: few-mode fibres (FMFs) and coupled-core multi-core (CC-MCFs). However, the multitude of spatial modes introduces new impairments, namely: group delay (GD) spread [2-4] given the interplay between differential mode delay (DMD) and linear mode coupling (LMC), intermodal nonlinear effects (IM-NL) [5-8], and mode dependent loss (MDL) [9, 10]. Recently, GD spread has been shown to be successfully mitigated using multi-input multi-output (MIMO) based DSP techniques [11, 12] and DMD compensation maps, for transmission over 1000s km [13, 14]. Currently, performance is mainly limited by prototype components MDL [15], and by fibre IM-NL interactions [16]. But given the continuous improvement of mode/core multiplexers (e.g. *MDL* < 0.5dB over the C+L band [17]) the impact of IM-NL will become dominant. Here we demonstrate the applicability of digital back propagation (DBP) to address the IM-NL penalties in SDM systems. After reviewing the models proposed to transmission in SDM fibres, we review our recent work [18] on simplified DBP methods for the different operational regimes determined by DMD and LMC.

2 Proposed Models

2.1 Transmission Modelling

In SDM systems transmission modelling involves solving a multimode nonlinear Schrödinger equation (NLSE), which can be written as [5-8]:

$$\partial_z A_{ui} + \overbrace{\left(\mathrm{j}\beta_{ui}^{(0)} + \beta_{ui}^{(1)}\partial_t - \frac{\mathrm{j}\beta_{ui}^{(2)}}{2}\partial_t^2 + \ldots + \frac{\alpha_{\mu i}}{2} \right)}^{=\hat{D}} A_{ui} = \overbrace{-\mathrm{j}\left[\gamma_{uuii}|A_{ui}|^2 + 2\gamma_{uvii}\sum_{v\neq u}|A_{vi}|^2 + \frac{2}{3}\gamma_{uvij}\sum_{v}|A_{vj}|^2 \right]}^{=\hat{N}} A_{ui} - \mathrm{j}\overbrace{\sum_{vk} C_{uvik} A_{vk} e^{\mathrm{j}\left(\beta_{ui}^{(0)} - \beta_{vk}^{(0)}\right)z}}^{=\hat{C}} \quad (1)$$

where i and j are mode u orthogonal polarizations. $A_{ui}(z,t)$, $\beta_{ui}^{(p)}$, and α_{ui} are the slowly varying field envelope, mode propagation constant p^{th}-derivative and attenuation, respectively. γ_{uvij} and C_{uvij} are the nonlinear and LMC coefficients, respectively, between ui and vj. $\hat{D}$, $\hat{N}$, and $\hat{C}$ are the dispersion, NL, and LMC operators, respectively. Given its impact on the efficiency of the IM-NL interactions, LMC has been under intensive research [19-21], both analytically and numerically. And, with practical fibres operating in all LMC regimes [22-27] a model capable of covering it all is convenient.

Analytically, and in the presence of extreme linear mode coupling regimes, it has been shown [5-7] that some or all the LMC terms in the multimode NLSE can be assumed to vary rapidly and seemingly randomly on a length scale that is expected to be short compared to the effective lengths associated with chromatic dispersion and the various manifestations of nonlinearity. Thus, like in SMFs and the well-known Manakov-PMD equations, one can average the propagation equation itself over all spatial modes. New Manakov equations were derived for SDM fibres with nonlinear coefficients averaged for the two extreme coupling regimes. In the weak coupling (WC) regime [6, 7], only the averaging over birefringence fluctuations must be considered, reducing the intramodal degeneracy factor to 8/9 and the intermodal degeneracy factor to 4/3, this is:

$$\hat{N} = -\mathrm{j}\left[\frac{8}{9}\sum_{k=\{i,j\}} \gamma_{uuik}|A_{uk}|^2 + \frac{4}{3}\sum_{\substack{v\neq u \\ k=\{i,j\}}} \gamma_{uvik}|A_{vk}|^2 \right] \quad (2)$$

In the strong coupling (SC) regime the averaging includes all modes [5], such that the nonlinear operator in (1) becomes:

$$\hat{N} = -\mathrm{j}\sum_{\substack{v \\ k=\{i,j\}}} \kappa|A_{vk}|^2, \quad \kappa = \frac{4}{3}\frac{2M}{2M+1}\left(\frac{1}{M^2}\sum_{u,v}\gamma_{uvvu} \right) \quad (3)$$

However, extension of analytical models above for the general case in terms of DMD and LMC is still under investigation [28].

Numerically, and in the strong regime, LMC is often modelled [7, 19, 20] using random unitary matrices in a multi-section fashion, where each section must be longer than the linear correlation length (as defined in [29]) – dubbed here as lumped-XT model. Unfortunately, this approach cannot be extended to the weak-to-intermediate LMC regime (with full mode mixing being achieved for more than 10 km) since nonlinear modelling requires a step-size much smaller than fibres nonlinear effective length (~20 km).

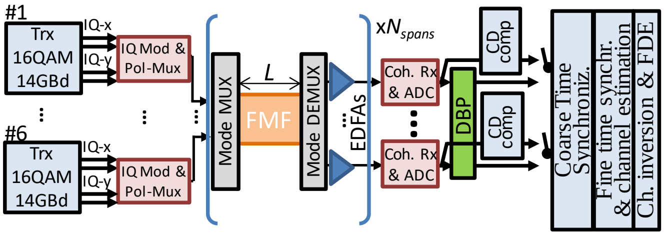

Fig. 1. Block diagram for system simulations using a fibre with 6 LP modes each with 2 orthogonal polarizations.

Table 1 Fibre Linear Characteristics at 1550nm

	LP01	LP02	LP11a	LP11b	LP21a	LP21b
GD [ps/km]	-0.29	-2.93	-0.66	-0.66	2.27	2.27
D [ps/(nm.km)]	22.18	21.55	22.15	22.15	21.84	21.84
S [fs/(nm^2.km)]	66.45	61.46	66.15	66.15	63.68	63.68

Recently, a semi-analytical LMC model capable of modelling mixing in a distributed fashion with an arbitrary step-size and applicable to all regimes has been developed [4] – dubbed here as distributed-XT model. Using such method, the authors matched the analytical predictions for GD statistics in FMF links and validate the GD spreading predictions for different coupling regimes and different link configurations [2, 4, 30]. Furthermore, using such model, the authors were able to accurately study for the first time the nonlinear distortion in FMFs operating in the intermediate coupling regime [14, 31].

2.2 Models Comparison

Here we review our recent comparison of the proposed models (discussed above) for full system simulation [29], this is: the WC-Manakov [6]; the SC-Manakov [5]; the distributed-XT model [4]; and the lumped-XT model [7]. To solve (1) we use a symmetric implementation of the split-step Fourier method [32] and select the step size by bounding the local error to be smaller than 10^{-5} (smaller values led to negligible change).

The simulation setup is shown in Fig. 1. A mode-division-multiplexing (MDM) system using a FMF with 6 linearly polarized (LP) modes (LP_{01}, LP_{02}, LP_{11a}, LP_{11b}, LP_{21a} and LP_{21b}) each with 2 orthogonal polarisations is considered. 672 Gbit/s per channel are transmitted in an optical super-channel with multiple WDM channels (per mode) modulated with 14 Gbaud polarisation-multiplexed 16QAM, 14.1 GHz spaced. The simulations here consider 2^{16} symbols per polarisation mode, and 2^{11} training symbols. After homodyne detection, the signals are sampled at 2 samples/symbol. The FMF used was optimised in [33] for low *DMD* (< 12 ps/km). Table 1 shows the linear characteristics at 1550nm, the *DMD* defined as max(*GD*)-min(*GD*) is 5.19 ps/km. Please see [33] for uncoupled NL coefficients. When considering different *DMD* values, we simply scale the GD vector in Table 1 instead of re-optimising the profile to avoid changing other fibre characteristics (as in [18]). For full details on the simulation setup, channel estimation and equalization please see [18]. Finally, after transmission, the *Q-factor* of the centre channel is estimated using the mean and standard deviation of the received symbols [34]. The figure of merit in the following is the minimum *Q-factor* among the 12 polarization modes guided.

Fig. 2 shows the *Q-factor* as a function of *XT* (i.e. LMC strength as defined in [4]) for 3 channels transmitted over 25 spans of 20km (following [35]) with -2 dBm/ch, in: (a) the

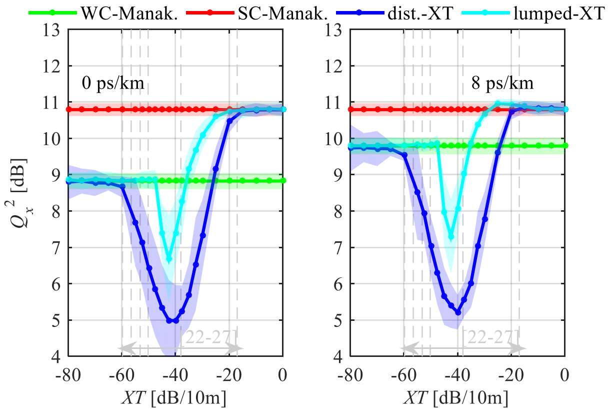

(a) (b)

Fig. 2. *Q-factor* as a function of *XT* for -2 dBm/ch and: (a) *DMD* = 0 ps/km, and (b) *DMD* = 8 ps/km. Lines shadow accounts for 3 times the standard deviation for 25 repetitions.

absence of DMD, and (b) the presence of a low *DMD*, 8 ps/km, confirming agreement with the Manakov models for the extreme LMC regimes. In Fig. 2 (a) and (b), two processes can be seen at work. Firstly, as the WC-Manakov approximation breaks down, phase rotations and partial averaging of the GDs introduced by LMC, allow intermodal FWM phase matching to be achieved for lower frequency separations and therefore for a broader range of frequency combinations than it would be possible in the absence of LMC – in this region performance degrades with increasing *XT* since there is no significant averaging of the nonlinear coefficients. Secondly, as the SC-Manakov regime is approached, fast random rotations of the hyper-polarization state of the field along the fibre length reduce the efficiency of the overall nonlinear process – in this region performance improves with increasing *XT* given the significant averaging of the nonlinear coefficients. Note that the intermediate coupling regime (-55 < *XT* [dB/10m] < -25) leads to worse performance than that of the WC and SC regimes, thus it should be avoided when attempting to minimise the nonlinear noise penalty. In any case, note that we considered an extreme-case scenario (3 channels only) in which the smallest frequency offset required for full intermodal phase matching in the weak coupling regime (22.2 GHz for *DMD* = 8 ps/km between LP_{01} and LP_{02}) is just above half of the signal bandwidth (21.2 GHz – as we are probing at the central channel). Such that as *XT* is increased and the variance of coupled GDs is reduced, some IM-FWM products from different fibre sections can now add up coherently. Furthermore, Fig. 2 shows that the lumped LMC model only captures the qualitative performance behaviour in both of these two processes, and is suitable only for system optimization as it accurately locates the locations of maximum performance and minimum performance.

Finally, the fully stochastic solution of (1) following the semi-analytical LMC modelling [4] is best suit to deliver accurate absolute performance prediction across all operation regimes. Therefore, appropriate to develop and characterise the performance of simplified DBP methods.

3 DBP Performance

Here we present DBP performance results for 19 channels and 12 spans of 20 km using as figure of merit the *Q-factor* of the

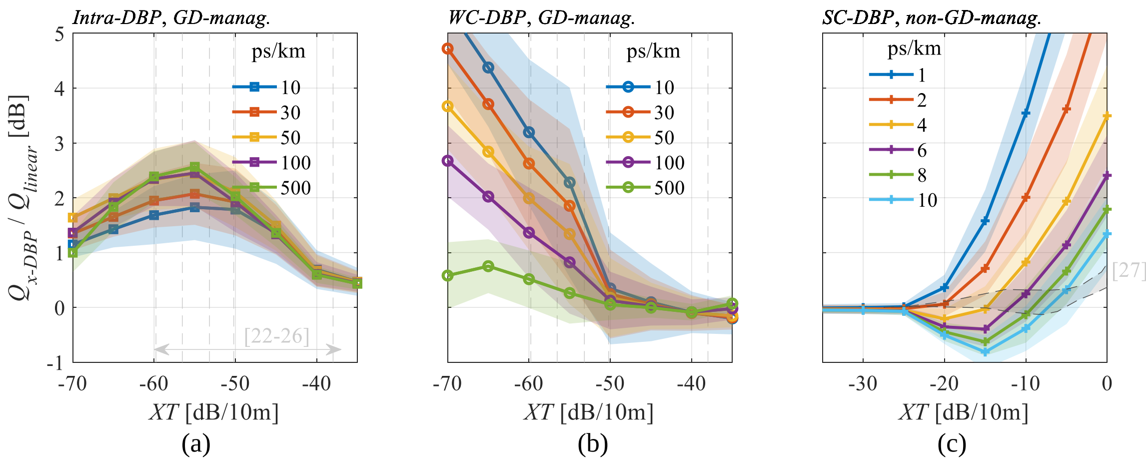

Fig. 3. *Q-factor* gain as a function of *XT* after 12×20 km, -2 dBm/ch and different *DMD* values, with: (a) Intra-DBP, (b) WC-DBP and (c) SC-DBP. Lines shadow accounts for 3 times the standard deviation for 100 repetitions.

centre channels averaged over the 12 polarisation modes. Including non-GD-managed and GD-managed spans (in the latter by cascading 2 fibres with opposite sign GD vectors). DBP is tested for 3 different sets of NL coefficients to best approximate the impact of LMC, namely the coefficients in: the WC-Manakov approximation (2) (WC-DBP), the SC-Manakov approximation (3) (SC-DBP), or just the intra-modal NL coefficients in WC-Manakov approximation (Intra-DBP). Note that when following the SC-Manakov approximation GD is nulled. Finally, to assess its full potential DBP considers the total number of channels being transmitted and a fixed step of 100 m (smaller step size led to negligible improvement).

Figure 3 shows the *Q-factor* improvement over linear equalisation as a function of *XT* after 240 km with different values of *DMD* and a launch power of -2 dBm/ch, for: (a) Intra-, (b) WC- and (c) SC-DBP. First, it can be seen that WC- and SC-DBP can provide significant compensation (above 1 dB) in the regimes where their Manakov equations are valid (for $XT < -50$ dB/10m and $XT > -25$ dB/10m, respectively). But, also that Intra-DBP provides a performance improvement in many cases higher than that of WC-DBP. Intra-DBP performs particularly well for sufficiently high *DMD* such that IM-NL distortion is not so dominant and for a range of low *XT* in which sufficient coupling events randomise a sufficient share of the IM-NL distortion. Thus, for sufficiently low *XT*, Intra-DBP gain rolls-off as can be seen in Figure 3 (a). In this way, for the WC-regime, with $-60 < XT$ [dB/10m] < -40 and $DMD > 30$ ps/km Intra-DBP provides the highest improvement between 1 and 3 dB, and for fibres with $XT < -50$ dB/10m and $DMD < 30$ ps/km WC-DBP provides an improvement between 1 and 4 dB. These *XT* and *DMD* ranges cover many the fibres presented in literature [22-25].

In the SC-regime, Fig. 3 (c) shows that SC-DBP can provide significant NL compensation for a significant range of uncoupled *DMD* and *XT* values. This range is better bounded by fibres spatial mode dispersion (SMD) [27] defined as the proportionality coefficient between the accumulated GD spread and the square root of propagation distance. Note that in the SC limit GD spread increases with the square root of the propagation distance [4], rather than linearly. In Fig. 3 (c) the dashed grey curves bound the possible working area (3 standard deviations) for the CC-MCF presented in [27] with a *SMD* of 3.14 ± 0.17ps/√km (average and standard deviation). Within such scenario performance improvement can reach 0.8 dB. Finally, Fig. 3 (c) shows that further *SMD* reduction in CC-MCFs can unlock a potential for 4dB improvement.

For intermediate *XT* none of the DBP approaches studied work even for negligible *DMD*. This is because for significant transmission distances (240 km, in this case) LMC leads to evolutions of the NL operator that differ significantly from that of the uncoupled operator and from the Manakov approximation. Outside the operational regime identified for WC- and SC-DBP, the evolution of the GD operator is no longer well approximated using the uncoupled GD coefficients, thus the NL distortion is either overcompensated or undercompensated when using the uncoupled NL coefficients.

4 Conclusion

Even for the complex spatial multiplexed systems significant performance improvement is possible using DBP provided that appropriate approximations for the effect of the stochastic nature of the LMC are considered. For example, fibres optimised primarily for low *XT* (and with intermediate-to-high *DMD*), including trench-assisted graded-index fibres [22] or multiple-step index fibres [36], allow a significant DBP gain if LMC is neglected. However, this signal processing approach gives no gain for high *XT* (and low *DMD*) fibres such as coupled-core fibres [27]. However, for such high *XT* fibres, if the LMC is averaged, the so called generalised Manakov approach, high performance gains are again possible. Whilst a small range of possible fibre parameters exist where the approximate models considered here failed to provide significant gain, and compensation would require continuous estimation of the random LMC, significant performance gains were possible for all possible XT and DMD regimes in which real fibres operate.

5 Acknowledgements

We thank Dr. Christian Sanchez for providing insight in to DSP development. This work has been supported by the Engineering and Physical Sciences Research Council (Grants EP/R024057/1-FPA-ROCS, EP/M005283/1-UPON, EP/L000091/1-PEACE). To access the underlying data see https://doi.org/10.17036/researchdata.aston.ac.uk.00000411.

6 References

[1] Richardson, D., Fini, J., Nelson, L.: 'Space-division multiplexing in optical fibres', Nature Photonics, 2013, 7, p. 354
[2] Ho, K., Kahn, J.: 'Linear Propagation Effects in Mode-Division Multiplexing Systems', J. Lightw. Technol., 2014, **32,** (4), pp. 614-628
[3] Antonelli, C., Mecozzi, A., Shtaif, M.: 'The delay spread in fibers for SDM transmission: dependence on fiber parameters and perturbations', Optics Express, 2015, 23, (3), pp. 2196-2202
[4] Ferreira, F., Costa, C., Sygletos, S., Ellis, A.: 'Semi-Analytical Modelling of Linear Mode Coupling in Few-Mode Fibers', J. Lightw. Technol., 2017, **35**, (18), pp 4011-4022
[5] Mecozzi, A., Antonelli, C., Shtaif, M., 'Nonlinear propagation in multi-mode fibers in the strong coupling regime', Optics Express, 2012, **20**, (11), pp. 11673-11678
[6] Mecozzi, A., Antonelli, C., Shtaif, M., 'Coupled Manakov equations in multimode fibers with strongly coupled groups of modes', Optics Express, 2012, **20**, (21), pp. 23436-441
[7] Mumtaz, S., Essiambre, R., Agrawal, G.: 'Nonlinear Propagation in Multimode and Multicore Fibers: Generalization of the Manakov Equations', J. Lightw. Technol., 2013, **31**, (3), pp. 398-406
[8] Ferreira, F., Jansen, S., Monteiro, P., Silva, H.: 'Nonlinear semi-analytical model for simulation of few-mode fiber transmission', IEEE Photon. Technol. Lett., 2012, **24**, (4), pp. 240-42
[9] Lobato, A., Ferreira, F., Kuschnerov, M., et al.: 'Impact of mode coupling on the mode-dependent loss tolerance in few-mode fiber transmission', Optics Express, 2012, **20**, (28), pp. 29776- 29783
[10] Ho, K.., Kahn, J.: 'Mode-dependent loss and gain: statistics and effect on mode-division multiplexing', Optics Express, 2011, **19**, (17), pp. 16612-16635.
[11] Costa, C., Ferreira, F., Suibhne, N.M., et al.: 'Receiver Memory Requirement in Mode Delay Compensated Few-Mode Fibre Spans with Intermediate Coupling', Proc. ECOC, Sept. 2016, p. Tu.1.E.4
[12] Arik, S., Askarov, D., Kahn, J.: 'Effect of Mode Coupling on Signal Processing Complexity in Mode-Division Multiplexing', J. Lightw. Technol., 2013, **31**, (3), pp. 423-431
[13] Ryf, R., Alvarado, J. C., Huang, B., et al.: 'Long-Distance Transmission over Coupled-Core Multicore Fiber', Proc. ECOC, Sept. 2016, p. Th.3.C.3
[14] Ferreira, F., Costa, C., Sygletos, S., Ellis, A.: 'Nonlinear Transmission Performance in Delay-Managed Few-Mode Fiber Links with Intermediate Coupling', Proc. OFC, March 2017, p. Th2A.53
[15] Rademacher, G., Ryf, R., Fontaine, N. K., et al.: 'Long-Haul Transmission over Few-Mode Fibers with Space-Division Multiplexing', J. Lightw. Technol., 2018, 36, **(6)**, pp. 1382-88
[16] Suibhne, N., Ellis, A., Gunning, F., Sygletos, S.: 'Experimental verification of four wave mixing efficiency characteristics in a few mode fibre', Proc. ECOC, Sept. 2013, p. P1.14
[17] Riesen, N., Gross, S., Love, J. D., et al.: 'Monolithic mode-selective few-mode multicore fiber multiplexers', Scientific Reports, 2017, **7**, (1), p. 6971
[18] Ferreira, F., Costa, C., Sygletos, S., Ellis, A., 'Overcoming degradation in spatial multiplexing systems with stochastic nonlinear impairments', Scientific Reports, 2018, **8,** (1), pp. 17539
[19] Ho, K.-P., Kahn, J.M., 'Statistics of Group Delays in Multimode Fiber With Strong Mode Coupling', J. Lightw. Technol., 2011, **29**, (21): pp. 3119-3128
[20] Mecozzi, A., Antonelli, C., Shtaif, M., 'Intensity impulse response of SDM links', Opt Express, 2015, **23**, (5): pp. 5738-43
[21] Rademacher, G., Warm, S., Petermann, K., 'Influence of Discrete Mode Coupling on the Nonlinear Interaction in Mode-Multiplexed Systems', IEEE Photon. Technol. Lett., 2013, **25,** (13), pp. 1203-1206
[22] Gruner-Nielsen, L., Sun, Y., Nicholson, J., et al.: 'Few Mode Transmission Fiber With Low DGD, Low Mode Coupling, and Low Loss', J. Lightw. Technol., 2012, **30**, (23), pp. 3693-3698
[23] An, L., Amin, A., Chen, X., Shieh, W.: 'Reception of mode and polarization multiplexed 107-Gb/s CO-OFDM signal over a two-mode fiber', Proc. OFC, March 2011, p. PDPB8
[24] Ryf, R., Randel, S., Gnauck, A., et al.: 'Mode-Division Multiplexing Over 96 km of Few-Mode Fiber Using Coherent 6 × 6 MIMO Processing', J. Lightw. Technol., 2012, **30**, (4), pp. 521-531
[25] Mori, T., Sakamoto, T., Wada, M., et al. 'Low DMD four LP mode transmission fiber for wide-band WDM-MIMO system', Proc. OFC, March 2013, p. OTh3K.1
[26] Ryf, R., Essiambre, R. J., Gnauck, A., et al.: 'Space-Division Multiplexed Transmission over 4200 km 3-Core Microstructured Fiber', Proc. OFC, March 2012, p. PDP5C.2
[27] Hayashi, T., Tamura, Y., Hasegawa, T., Taru, T.: 'Record-Low Spatial Mode Dispersion and Ultra-Low Loss Coupled Multi-Core Fiber for Ultra-Long-Haul Transmission', J. Lightw. Technol., 2017, **35**, (3), pp. 450-457
[28] Buch, S., Mumtaz, S., Essiambre, J.: 'Averaged nonlinear equations for multimode fibers valid in all regimes of random linear coupling', Opt Fiber Technol, 2019. 48, pp. 123-127
[29] Ferreira, F., Sanchez, C., Sygletos, S., Ellis, A.: 'Nonlinear Performance of Few-Mode Fiber Links With Intermediate Coupling', J. Lightw. Technol., 2019, **37**, (3) pp. 989-999
[30] Arik, S., Ho, K., Kahn, J.: 'Delay Spread Reduction in Mode-Division Multiplexing: Mode Coupling Versus Delay Compensation', J. Lightw. Technol., 2015, **33,** (21), pp. 4504-12
[31] Ferreira, F., Sanchez, C., Sygletos, S., Ellis, A.: 'Advantages of strong mode coupling for suppression of nonlinear distortion in few-mode fibers', Proc. OFC, March 2016, p. Tu2E.3
[32] Sinkin, O., Holzlohner, R., Zweck, J., Menyuk, C.: 'Optimization of the split-step fourier method in modeling optical-fiber communications systems', J. Lightw. Technol., 2003, **21**, (1), pp. 61-68
[33] Ferreira, F., Fonseca, D., Silva, H.: 'Design of Few-Mode Fibers With M-modes and Low Differential Mode Delay', J. Lightw. Technol., 2014, **32** (3), pp. 353-360
[34] Schmogrow, R., Nebendahl, B., Winter, M., et al.: 'Error Vector Magnitude as a Performance Measure for Advanced Modulation Formats', IEEE Photon. Technol. Lett., 2012, **24**, (1), pp. 61-63
[35] Doran, N., Ellis, A.: 'Minimising total energy requirements in amplified links by optimising amplifier spacing', Optics Express, 2014, **22**, (16), pp. 19810-19817
[36] Sakamoto, T., Mori, T., Yamamoto, T., Tomita, S.: 'Differential Mode Delay Managed Transmission Line for WDM-MIMO System Using Multi-Step Index Fiber', J. Lightw. Technol., 2012, **30**, (17), pp. 2783-2787